Remote Sensing of Environment 181 (2016) 151–161

Contents lists available at ScienceDirect

Remote Sensing of Environment

journal homepage: www.elsevier.com/locate/rse

Spatiotemporal variations in surface velocity of the Gangotri glacier, Garhwal Himalaya, India: Study using synthetic aperture radar data

S.P. Satyabala

Divecha Centre for Climate Change, Indian Institute of Science, Bangalore 560012, India

ARTICLE INFO

Article history:
Received 18 September 2015
Received in revised form 10 March 2016
Accepted 31 March 2016
Available online xxxx

Keywords:
Glacier velocity
Gangotri glacier dynamics
Garhwal Himalaya
Seasonal fluctuations
Interannual fluctuations
SAR
PALSAR
ASAR

ABSTRACT

The Gangotri glacier is the largest in the Garhwal Himalaya, India and its melt water forms the main source stream of the Ganga River, yet its dynamics are poorly understood. Its long record of terminus retreat measurements (1800–present) shows multi-decadal oscillations and more recently a slowing down of the retreat. Its complex dynamics are also indicated by studies of proglacial melt–water at the terminus. However, there have been no systematic measurements of its surface velocity or how it changes seasonally or over longer-term time scales. Here, I have characterized the spatiotemporal variations of surface velocity of the Gangotri glacier using synthetic aperture radar (SAR) data spanning nearly two decades (1991–2011).

The main findings are as follows: (1) The glacier undergoes seasonal fluctuations in surface velocities: there was a clear summer speedup of ~57%–126% compared to winter velocities between 0 and 12.6 km from the terminus, with peak summer speeds of 63.1 ± 5.4 m/yr in 1992, 66.6 ± 6.0 m/yr in 1999, 58.2 ± 4.5 m/yr in 2004 and 42.8 ± 4.2 m/yr in 2007 whereas winter speeds were relatively stable (25–30 m/yr) during the same period. This summer speedup is indicative of increased basal sliding, known to occur when melt–waters penetrate to the glacier bed resulting in reduced friction. (2) These summer velocities exhibited an inter-annual reduction, which was manifest as a reduction in summer speed up from >120% in 2004 to <60% in 2007. This pattern continued into 2011, despite the availability of abundant melt–water during those years. This inter-annual reduction indicates the formation of increasingly efficient melt–water channels year on year resulting in lesser lubrication at the glacier–bed interface.

My results show that the Gangotri glacier is dynamic throughout its length with systematic spatiotemporal variations in surface velocity that elucidate its subglacial processes. Based on my results and other evidence in the literature, I propose that the subglacial drainage system of the Gangotri glacier is subject to seasonal and inter-annual hydrodynamic coupling between winters and melt-seasons akin to other glaciers.

1. Introduction

The Gangotri glacier originates in the Chaukhamba massif, a ridge formed by four mountains with the highest peak at 7138 m asl (Fig. 1). The glacier flows northwest towards Gaumukh for about 30 km, fed by several tributary glaciers on either side. It terminates at Gaumukh ~ 4 km asl (Bhambri, Bolch, & Chaujar, 2012) feeding its melt-water into the Bhagirathi River, the main source stream of the sacred Ganga River. Its present day equilibrium line altitude was estimated to be 5560 m (Naithani, Nainwal, Sati, & Prasad, 2001). Nearly a third of the glacier area is covered by debris (Bhambri, Bolch, & Chaujar, 2011b; Bhambri, Bolch, Chaujar, & Kulshreshtha, 2011a; Scherler, Bookhagen, & Strecker, 2011a). In optical images, debris cover can be seen to a distance of ~ 13 km from the terminus, followed by a transition zone with partial debris and clean ice/snow cover from ~ 17 km from the terminus until the head of the glacier.

Gangotri glacier has one of the longest records of terminus retreat measurements in the Himalayan region (1842–present) at rates of ~20–30 m/yr with multi-decadal variations and this retreat is reported to have reduced/stopped in the last decade (Srivastava, 2012; Kumar, Dumka, Miral, Satyal, and Pant (2008); Raina, 2009; Bhambri & Bolch, 2009; Bhambri et al., 2012; Kargel, Cogley, Lenoard, Haritashya, & Byers, 2011; Scherler et al., 2011a; Puneet Saraswat et al., 2013). Other studies indicate mass loss in recent years (Bhambri et al., 2012; Kääb, Etienne, Christopher, Julie, & Yves, 2012; Kargel et al., 2011; Raina, 2009; Scherler et al., 2011a). Kargel et al. (2011) infer that the Gangotri glacier "and probably most other large Himalayan glaciers will likely shrink dramatically this century, with thinning of debris-covered tongues and supraglacial lake growth helping to drive the retreat".

Comprehensive glaciological and mass-balance studies have not been carried out for the Gangotri glacier due to its inaccessibility (Srivastava, 2012). With the exception of the Siachen glacier (which is 73 km long and has been studied using the hydrological method), most of the glaciers in the Indian Himalaya for which in-situ mass balance studies were carried out are relatively small mostly being ~5–

E-mail address: satyabala@gmail.com.

http://dx.doi.org/10.1016/j.rse.2016.03.042

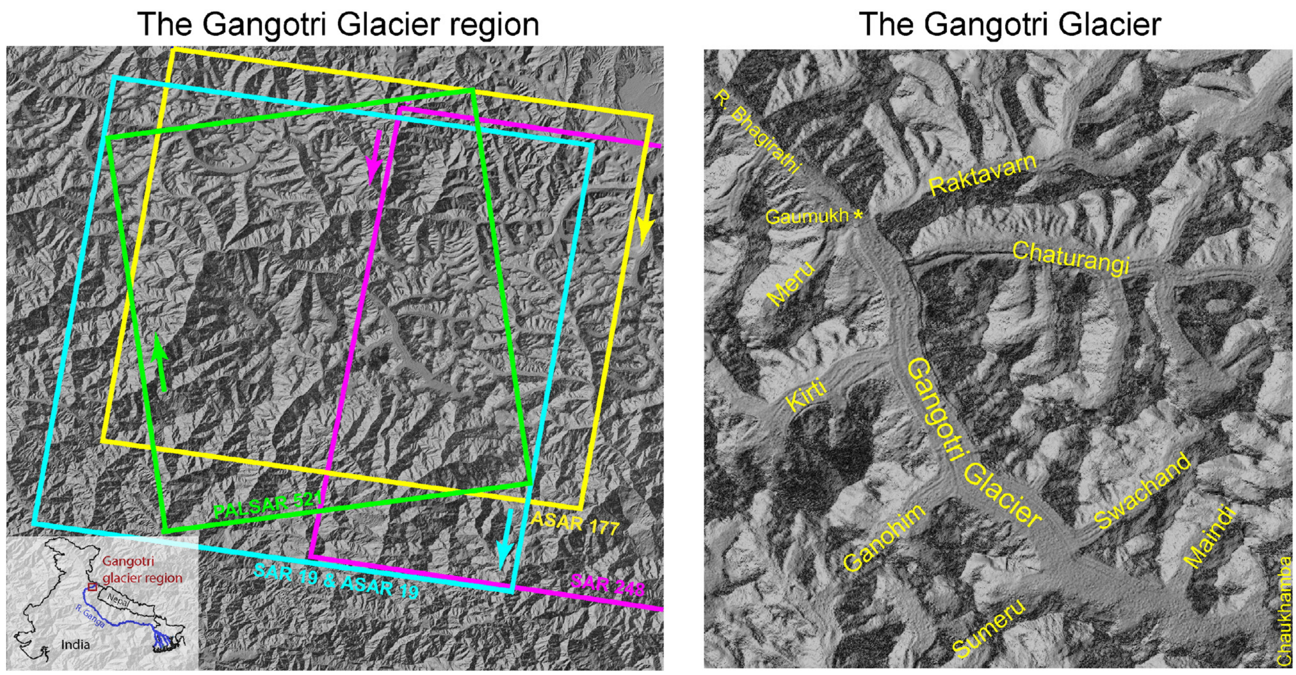

Fig. 1. The Gangotri glacier. *Left*: A shaded relief map (DEM) of the Gangotri glacier region, with inset showing its geographical location in India. Rectangles marked on the figure indicate satellite tracks with track direction marked by arrows. *Right*: Close-up of the Gangotri glacier with its major tributaries marked. The glacier originates near Chaukhamba (*bottom right*) and flows towards its terminus, Gaumukh, the source of the Bhagirathi river.

7 km length (Pratap, Dobhal, Bhambri, Mehta, & Tewari, 2015). The only other clues to the dynamics of the Gangotri Glacier come from studies of suspended sediment concentration in melt–water carried by its proglacial stream (Haritashya, Kumar, & Singh, 2010; Haritashya, Singh, Kumar, & Gupta, 2006; Singh, Haritashya, Kumar, & Singh, 2006).

More recently, measurements of surface velocity of glaciers have been possible with the availability of remote sensing data and yielded a number of interesting insights into their dynamics (Copland et al., 2009; Kääb, 2005; Quincey, Luckman, & Benn, 2009b; Scherler & Strecker, 2012; Yasuda & Furuya, 2013). While a number of velocity measurements have been made for the Gangotri glacier (Vijay Kumar, Venkataraman, Høgda, & Larsen, 2013; Scherler, Leprince, & Strecker, 2008; Scherler, Bookhagen, & Strecker, 2011b; Gantayat, Kulkarni, & Srinivasan, 2014), we know very little about their temporal variations, whether seasonal or longer-term.

Here, I have systematically characterized for the first time, spatial and temporal variations of the surface velocity of the Gangotri glacier using SAR data spanning nearly two decades (1992–2011). These results reveal a dynamic Gangotri glacier with both seasonal and inter-annual velocity variations that provide insights into its underlying dynamics.

2. Data & methods

A total of 65 SAR images from 5 satellites spanning the period of 1991–2011 were used in this study (Table 1, Fig. 1, Table S1). All data were processed from raw Level-0 (ERS1/2& ENVISAT) and Level-1.0 (ALOS-PALSAR). I used pixel-offset-tracking (intensity tracking or speckle tracking) based on maximizing the cross-correlation of SAR image patches (Pritchard, Murray, Luckman, Strozzi, & Barr, 2005; Strozzi, Luckman, Murray, Wegmüller, & Werner, 2002) to estimate glacier velocities for pairs of images acquired at different times. A total of 270 pairs were processed of which 147 (Table S2) have been selected for the analysis presented here. As the study area consists of high mountainous region in the Himalaya, I used DEM-assisted co-registration of the SAR images to minimize stereoscopic artifacts in offset-tracking displacements due to high topography (Kobayashi, Takada, Furuya, & Murakami, 2009). I have used voids filled SRTM-DEM (NASA's Shuttle Radar Topography Mission) with 3 arcsec resolution (Jarvis, Reuter, Nelson, & Guevara, 2008).

Offset tracking yields two dimensional maps of glacier displacement that may have occurred in the time interval between the acquisition of the image pairs from which glacier velocity may be derived assuming

Table 1
SAR satellites used in this study for offset-tracking data/velocity maps.

Sensor, track, mode	Wavelength, frequency band, repeat cycle, incidence angle, pixel spacing (range × azimuth)	Tracking window size pixels in range × azimuth	Step size pixels in range × azimuth	Mean offset bias m/yr	Time periods, number of images
ENVISAT ASAR, 177, IS6	5.6 cm, C band, 30 days, 40°, 7.8 m × 3.84 m	64 × 320	8 × 40	2–4 ± 4	2010–2011, 5
ALOS PALSAR, 521, FBS & FBD	23.5 cm, L band, 46 days, 38°, 4.67 m × 3.15 m	80 × 400	16 × 32	0.5–4 ± 3	2007–2011, 13
ENVISAT ASAR, 19, IS2	5.6 cm, C band, 35 days, 23°, 7.8m × 4.06 m	48 × 240	8 × 40	2–7 ± 5	2004–2007, 13
ERS 1/2 SAR, 19, IS2	5.6 cm, C band, 35 days, 23°, 7.9 m × 3.99 m	48 × 240	8 × 40	2–6 ± 3	1992–1993 & 1998-1999, 16
ERS 1/2 SAR, 248, IS2	5.6 cm, C band, 35 days, 23°, 7.9 m × 3.99 m	48 × 24l0	8 × 40	1–6 ± 4	1992–1993 & 1998-1999, 18

that the glacier flows parallel to the surface and in the direction of maximum surface slope (Strozzi et al., 2002). The above mentioned SRTM DEM was used to obtain the Gangotri glacier geometry. The measured velocity vectors align nearly parallel to the margins of the glacier (Fig. 2). The correlation signal-to-noise ratio (SNR) was used to measure the quality of offsets. The size of the image patches used for cross-correlation (hereafter, window size) is an important parameter: the window must be large enough to contain intensity features required to match the two images and sufficiently small so as to not blur the result (Table 1; Supplementary Section S1).

Typically image pairs with smallest temporal separation are used in order to minimize loss of signal due to changes in the scattering properties of the objects (Yasuda & Furuya, 2013). However, larger temporal separations are more suitable for debris-covered areas like the Himalayan region. The supra-glacial debris on glaciers is stable and forms distinct surface features/patterns that enable the use of images pairs with longer time intervals up to 6-months to several years (Kääb, 2005; Luckman, Quincey, & Bevan, 2007; Quincey et al., 2009b). I could obtain offset-tracking displacement maps with temporal baselines of several years but used baselines <400 days in order to preserve temporal resolution. In the case of ERS-1/2 &ENVISAT-ASAR I2-mode data, small temporal separations of 35-day (orbital repeat interval) often yielded very noisy offset-tracking results and hence we avoided these pairs. On the other hand, ENVISAT-ASAR track 177 I6-mode 30-day pairs and ALOS-PALSAR 46-day pairs had a good signal to noise ratio probably due to their larger incidence angles (~40°) compared to ERS-1/2 and ENVISAT I2-modes with lower incidence angles (~23°). Even the non-debris covered regions (here mostly the accumulation zone) could be tracked fairly well especially in winter, perhaps because the cold environment and high basal sliding contribute to the

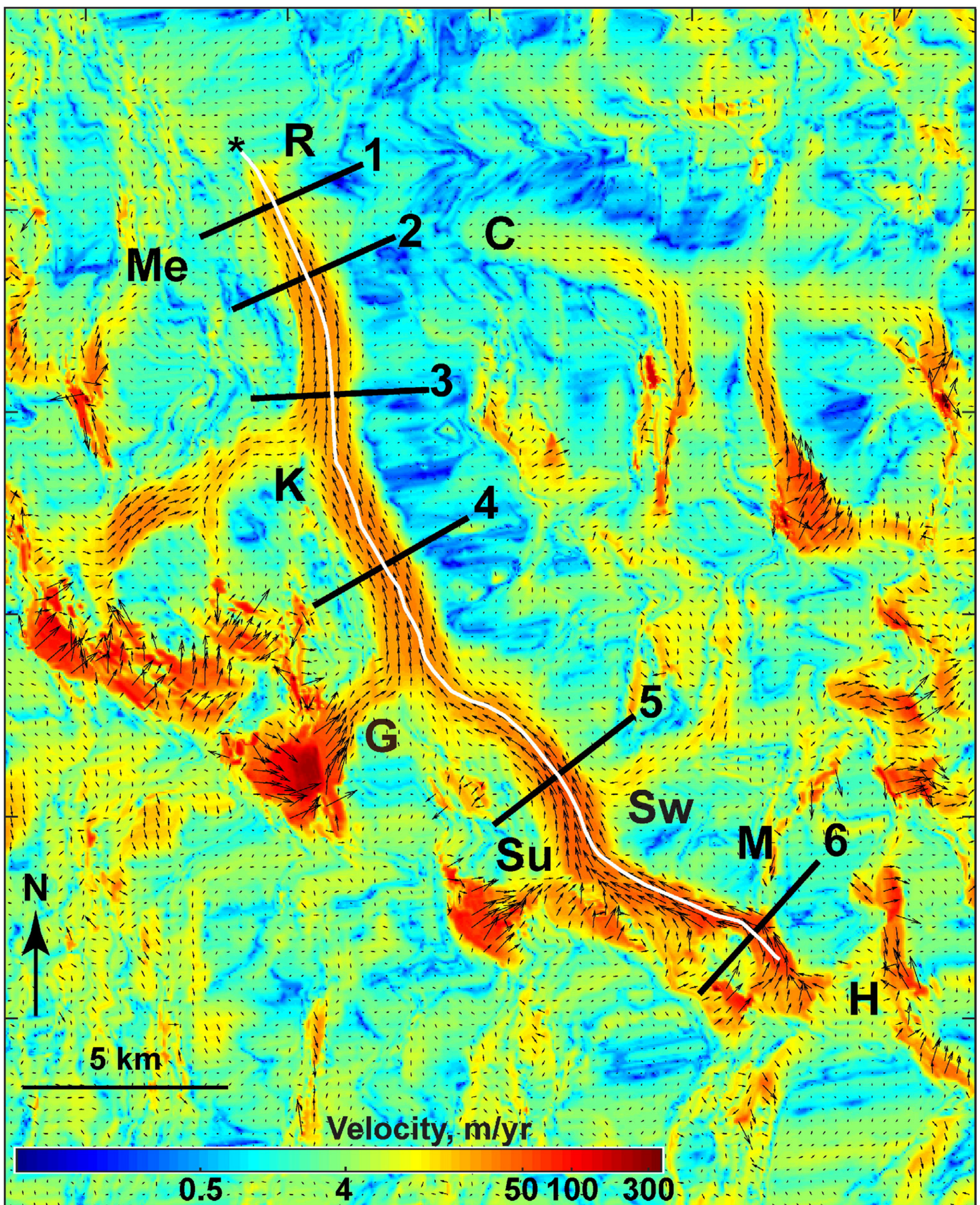

Fig. 2. Winter surface velocity map for the Gangotri glacier and its tributaries in 2008 (based on images acquired on 5 Feb & 22 March 2008, 46 days interval). Colors indicate the magnitude of velocity and vectors indicate direction. The centerline of the Gangotri Glacier is indicated by the white line and locations of across-glacier profiles used in later figures are indicated by black lines with numbers. The major tributaries are marked with letters (R: Raktavarn, Me: Meru, C: Chaturangi, K: Kirti, G: Ganohim, Su: Sumeru, Sw: Swachhand, M: Maiandi). The asterisk marks the terminus (Gaumukh, the source of the Bhagirathi River), and H marks the head of the Gangotri glacier (the Chaukhamba massif is on its right). See Fig. S1 for a map of standard deviation of surface velocity measurements.

preservation of ice surface structures over time (Kääb, 2005). However, surface melting and snowfall can obscure stable features. Glaciers in this region (Garhwal) are fed both by winter and summer accumulation (Bhambri et al., 2011a). Snowfall affects tracking efficiency to different extents with the L-band and C-band data. Deeper penetration of L-band data, compared to C-band, into snow and ice (Kääb et al., 2012; Rignot, Echelmeyer, & Krabill, 2001) enables more robust tracking of stable features. On the other hand, surface melting can cause spurious signals with physically unrealistic magnitudes and/or orientation of the displacement vectors and affects both L- and C-band data. All these factors resulted in usable velocities only within ~12 km up-glacier in the ablation region during summers and up to ~25 km up-glacier into the accumulation region during winters. The results from the different SAR satellite data used in this paper are comparable as also found by others who tried to extend the analysis to longer temporal periods (Yasuda & Furuya, 2013). This was checked by using temporally overlapping image pairs, where available.

2.1. Error analysis and noise filtering

The cross-correlation peak signal-to-noise ratio (SNR) is used to reject poor matches in offset-tracking. Typically SNR values > 4.0 are acceptable which translates to a precision in offset-tracking shift accuracy of 1/20th of a pixel (Strozzi et al., 2002). This shift accuracy translated to velocity measurement amounts to an accuracy that is smaller for longer temporal separation. However, errors (SNR) in offset-tracking results are larger and usually estimated empirically by considering shifts (expected to zero) over stationary areas in the vicinity of the glacier. Additionally, a direction filter is used to reject false offsets (Pritchard et al. 2005). I used a filter that rejects displacements with the SNR < 4 and direction vectors that are not oriented within 35° (25° for PALSAR data) degrees from the glacier flow direction. Offset biases ranged from 0.5 to 7 m/yr in off-glacier areas, being larger in summer pairs than winter pairs and were the smallest in PALSAR data (Table 1). These values are much less than the glacier velocities that span 20–70 m/yr for the Gangotri glacier. Similar uncertainties were obtained in other mountainous regions e.g. in Karakorum, Pakistan (Quincey et al., 2009a), in Nepal (Luckman et al., 2007) and in Kunlun Shan, NW Tibet (Yasuda & Furuya, 2013).

3. Results

Surface velocity maps for the Gangotri glacier were obtained from 147 offset-tracking image pairs spanning 1992–2011. The estimated velocity for each pair represents the average velocity of the Gangotri Glacier during the time period covered between these two images. These intervals frequently include both summer (April–September) and winter (October to March) months of a year, in different proportions, depending on the satellite image acquisition dates (not synchronized to the hydrological year) but with overlapping time intervals to form a fairly well covered temporal series particularly in periods of dense sampling such as 1992–93, 2004–2005, 2007–2008, including annual velocities. We therefore categorized the intervals into three groups: (1) *summer data*: those that included a large proportion of summer (>60%), (2) *winter data*; those that contained a large proportion of winter (>60%) and (3) *remaining data*: with roughly equal proportions of summer and winter months.

I analyzed these maps for stable spatial patterns, as well as for seasonal and inter-annual fluctuations over the observation period, as detailed in the sections below.

3.1. Surface velocity maps: spatial variation — stable features

Surface velocity maps obtained during the winter months (October–March) revealed steady patterns from year to year in contrast to the summer velocity maps that are more variable. These steady patterns were highly repeatable and were strongly correlated with topographic features of the glacier. Fig. 2 shows a representative velocity map of the Gangotri glacier and its tributaries. There is a striking alignment of the flow vectors along the direction of flow of the main glacier from the head all the way to the terminus and the major tributaries are seen to be feeding into the Gangotri glacier (Figs. 2–3). The non-glaciated regions have much smaller velocities with large scatter in orientation.

3.1.1. Velocity variation along the glacier

The magnitude of surface velocity varies systematically along the length of the glacier (Fig. 4). While the velocity in general increases from the terminus to ~26 km up-glacier, there are significant variations. The velocity increases rapidly from ~5 to 10 m/yr within 0.5 km of the terminus to ~28 m/yr at ~4 km from the terminus. Thereafter the velocity is relatively stable at ~20–35 m/yr till ~13 km (Fig. 4). Further up-glacier the fluctuations are much larger, showing peaks of ~47 m/yr at 18 km and ~70 m/yr at 25 km up-glacier, which may be correlated with the tributaries feeding the glacier. Similar reduction of velocity along the main glacier before a confluence and an increase downstream has been observed before (Gudmundsson, Iken, & Funk, 1997b; Quincey et al., 2009b) and is replicated by models in which there is significant ice discharge from the tributary into the main glacier (Gudmundsson, 1997a). The stable variations stand in contrast to glaciers in the Karakorum region, where substantial fluctuations of high velocity also occur unrelated to the presence of tributaries (Copland et al., 2009; Kennet, 2014), sometimes on surge type glaciers, indicative of complex and unstable dynamics (Kennet, 2014).

3.1.2. Velocity variation across the glacier

The shapes of across-glacier surface velocity profiles have been used to infer the mechanism of flow of a glacier. The roughly parabolic across-glacier winter velocity profiles are indicative of predominant internal deformation (Fig. 4; Fig. S6; Quincey et al., 2009a; Quincey et al., 2009b; Copland et al., 2009), although there could still be significant basal sliding near the center of the glacier (Harbor, 1992; Rabus & Fatland, 2000).

3.1.3. Confluence of tributaries

Active tributaries (Kirti, Ganohim and Sumeru on the left margin and Swachhand and Maiandi glaciers on the right margin) show significant velocity at the confluence with the main Gangotri Glacier (Figs. 2, 3A–B). The velocity vectors maintain their streamlines for some distance downstream of the confluence, consistent with the medial moraines downstream of the confluence maintaining their identity for significant distance along the Gangotri glacier (Naithani et al., 2001; Srivastava, 2012). As expected, the Raktavarn, Meru and Chaturangi glaciers, that are known to have separated from the Gangotri glacier, show near-zero velocities between their snouts and the main trunk of the Gangotri glacier (Fig. 2).

3.2. Surface velocity: temporal variations

The Gangotri glacier exhibited intra-annual (short-term /seasonal) as well as inter-annual (long-term) changes in surface velocities.

3.2.1. Short term fluctuations: summer speedup

Fig. 4 shows representative along-glacier velocity profiles for two periods during the winter of 2008 (5 Nov 2007–5 Feb 2008 and 5 Feb–22 Mar 2008) and for the preceding summer of 2007 (5 May–5 Aug 2007). The surface velocity increases in summer (*summer speedup* is >50% of the winter velocity), become noisier with distance up-glacier as discussed in Section 2 and supplement S1. Therefore the analyses below are largely restricted to the debris-covered zone, although summer speedup can be recognized till 20 km up-glacier (Fig. 4). Summer speedup indicates increased and predominant basal sliding, based

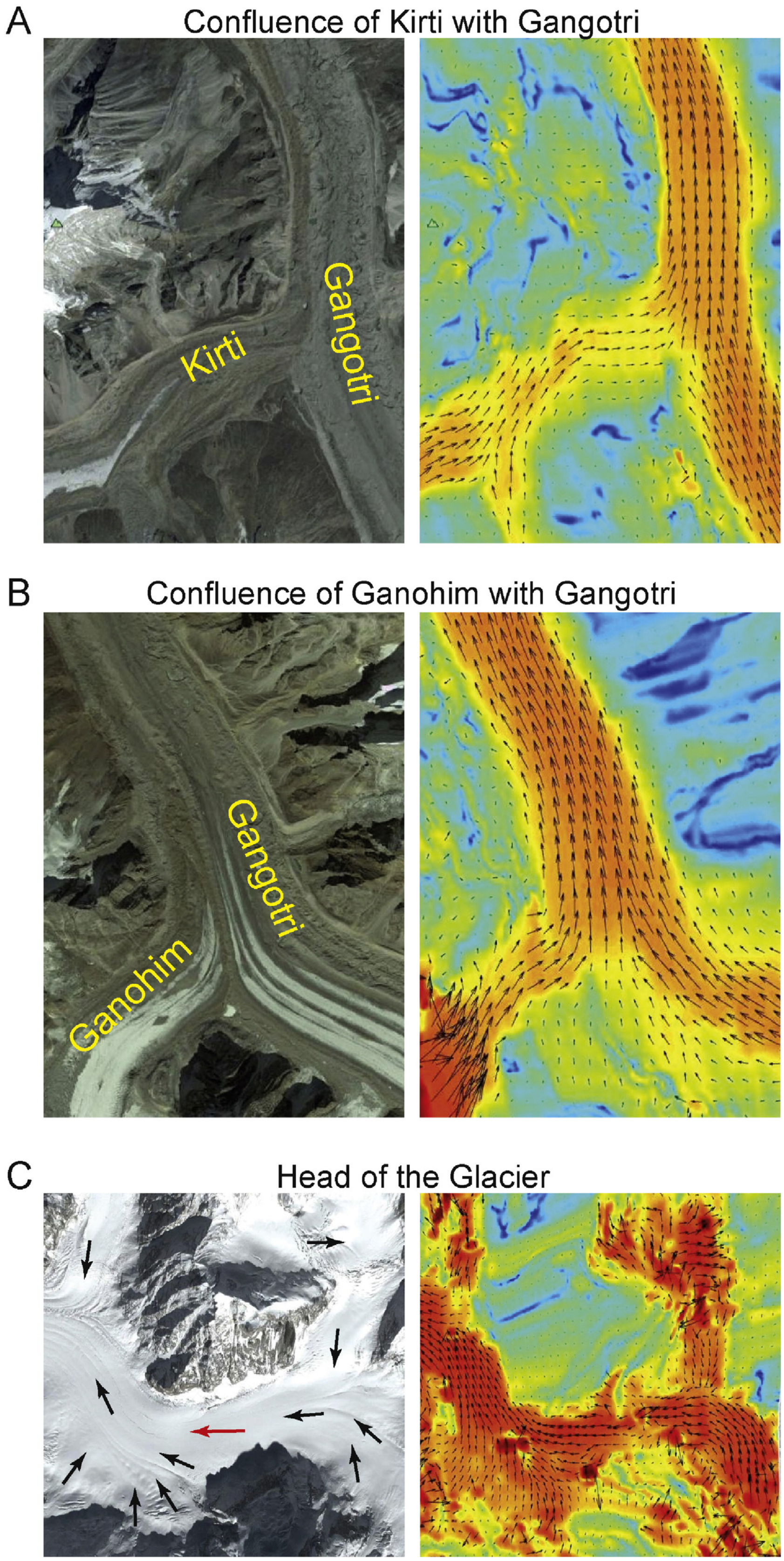

Fig. 3. Confluence of tributaries. A. Surface velocity variations near the confluence of Kirti tributary with Gangotri. The velocity vectors of both Gangotri and its tributary Kirti continue further downstream (northwards) of their confluence (*right*). On the *left* is shown a Google Earth image of approximately the same area where the medial moraines can be seen. B. Surface velocity variations near the confluence of Ganohim tributary with Gangotri. The velocity vectors of both Gangotri and its tributary Ganohim continue further downstream (northwards) of their confluence (*right*). On the *left* is shown a Google Earth image of the same area where the medial moraines can be seen. C. Surface velocity variations near the head of the Gangotri glacier. The arrows in the Google Earth image (*left*) indicate the major directions of flow corresponding to converging tributaries observed in the surface velocity map (*right*). The red arrow indicates the flow vector obscured in Fig. 1A due to signal loss but flow vectors are resolved here using offset tracking with a smaller window size (Supplementary Section S1).

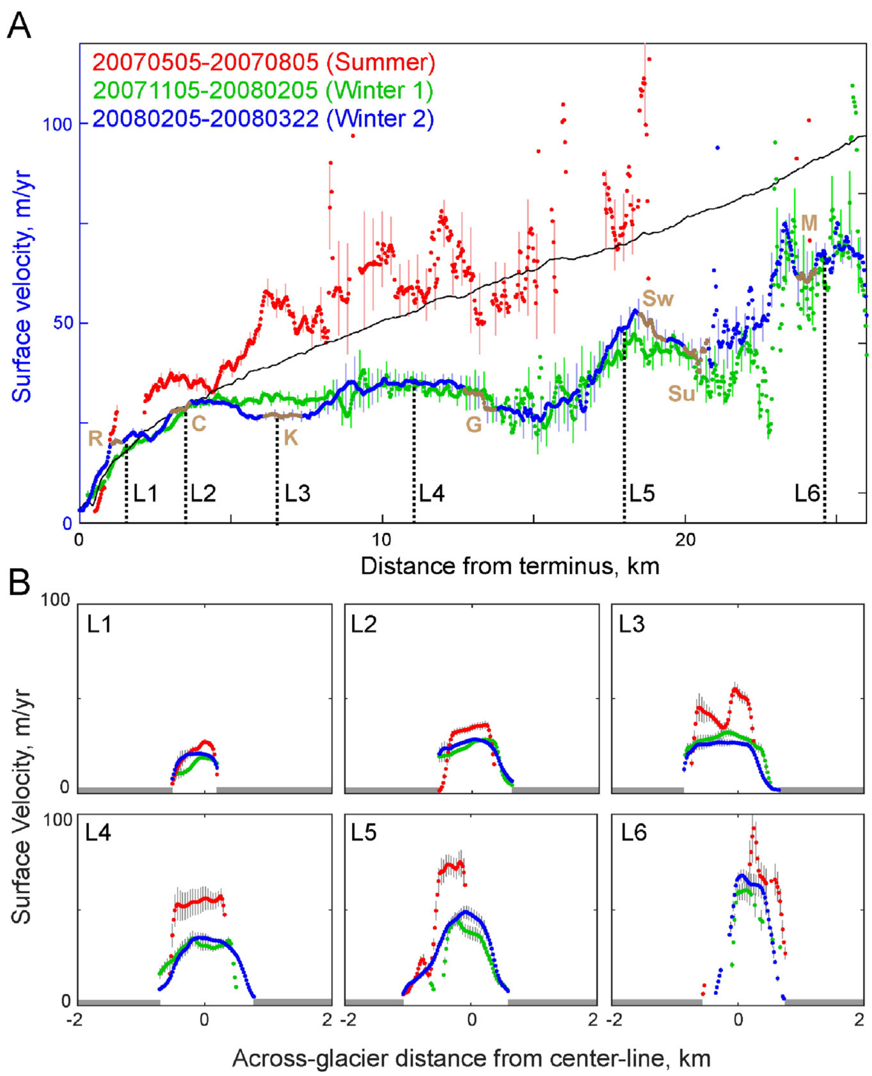

Fig. 4. Representative summer and winter surface velocity profiles for the Gangotri glacier. (A) Surface velocity profile along the centerline in Fig. 2 is plotted for one winter pair (*blue*), and for a summer pair (*red*) and a pair from the following winter (*green*). Image dates are shown in the legend. *Brown* regions on the *blue* winter profile indicate the approximate confluence of the marked tributaries. Elevation is indicated in *black*. Error bars represent standard deviations of the measurements obtained from the cross-correlation peak SNR (see Data and methods), but are shown only for a subset of points to avoid crowding. (B) (L1)–(L6) Surface velocity profiles across the centerline of the glacier for the locations in (A). Legend as in (A). Velocities with low SNR or with poor alignment with glacier margins have been masked (see section on error analysis). Thick grey bars on the x-axis represent non-moving areas outside the margin of the glacier. Note that the apparent truncation of summer profiles between the glacier margins indicates loss of data — see Supplementary Section S1 on window sizes).

primarily on the fact that these are on the seasonal / intra-annual time scale (Willis, 1995). Summer velocities were characterized by a sharp rise at the margins to a relatively flat/tilted profile in the center (Fig. 4; Fig. S6), also indicative of predominant basal sliding. This stands in contrast to the winter profiles discussed above which show parabolic profiles indicative of predominant internal deformation. An overview of spatial and temporal fluctuations of the velocity data obtained in this study are shown in Fig. 5.

The summer/winter pattern, an example of which is shown in Fig. 4, was not only present in each year but, where data was available, also evolved over time. To quantify the temporal evolution of summer/winter velocities, the average velocity along the glacier from the terminus to 12.6 km up-glacier (corresponding to the debris-covered part of the glacier) for each time interval, is shown in Figs. 6–7 (also Fig. S3) for time periods containing a number of measurements with overlapping time intervals covering different proportions of summer/winter months.

The first time period 1992–1993 (Fig. 6), reveals a gradual build-up of velocity towards the summer peak (63.1 ± 5.4 m/yr in 1992) followed by a decline to steady-state winter levels (29.4 ± 2.6 m/yr during 1992–93): a summer speedup of 114%. The winter velocity was 33.5 ± 2.9 m/yr in 1998 and the summer velocity was 66.6 ± 6.0 m/yr in 1999: a summer speedup of 99% (Fig. 5 and Fig. S3). The second time period 2004–2011 (Fig. 7), shows a similar pattern with peak summer velocities of 58.2 ± 4.5 m/yr in 2004 and 42.8 ± 4.2 m/yr in 2007 while the lowest winter velocities were 25.7 ± 2.3 m/yr in 2004–5 and 26.9 ± 1.9 m/yr in 2007–8, i.e. a speedup of 126% in 2004 but merely 59% in 2007.

3.2.2. Long term trend: inter-annual fluctuations

Besides the seasonal fluctuations, there is also a long-term pattern of decreasing summer velocities over the entire time period. The peak summer speed up of more than double the winter speeds during 1992, 1999 and 2004 reduced to <60% in 2007 with further reduction in the following years till 2011 (Fig. 7). This inter-annual trend of reducing summer velocities over a period of ~7–8 years starting in 2004 is also seen in the annual velocities, which would represent an average over the winter and summer periods. Due to data gaps and paucity of sampling during the years before 2004, it is unclear whether or not such a trend occurred during the period following the peaks in 1992

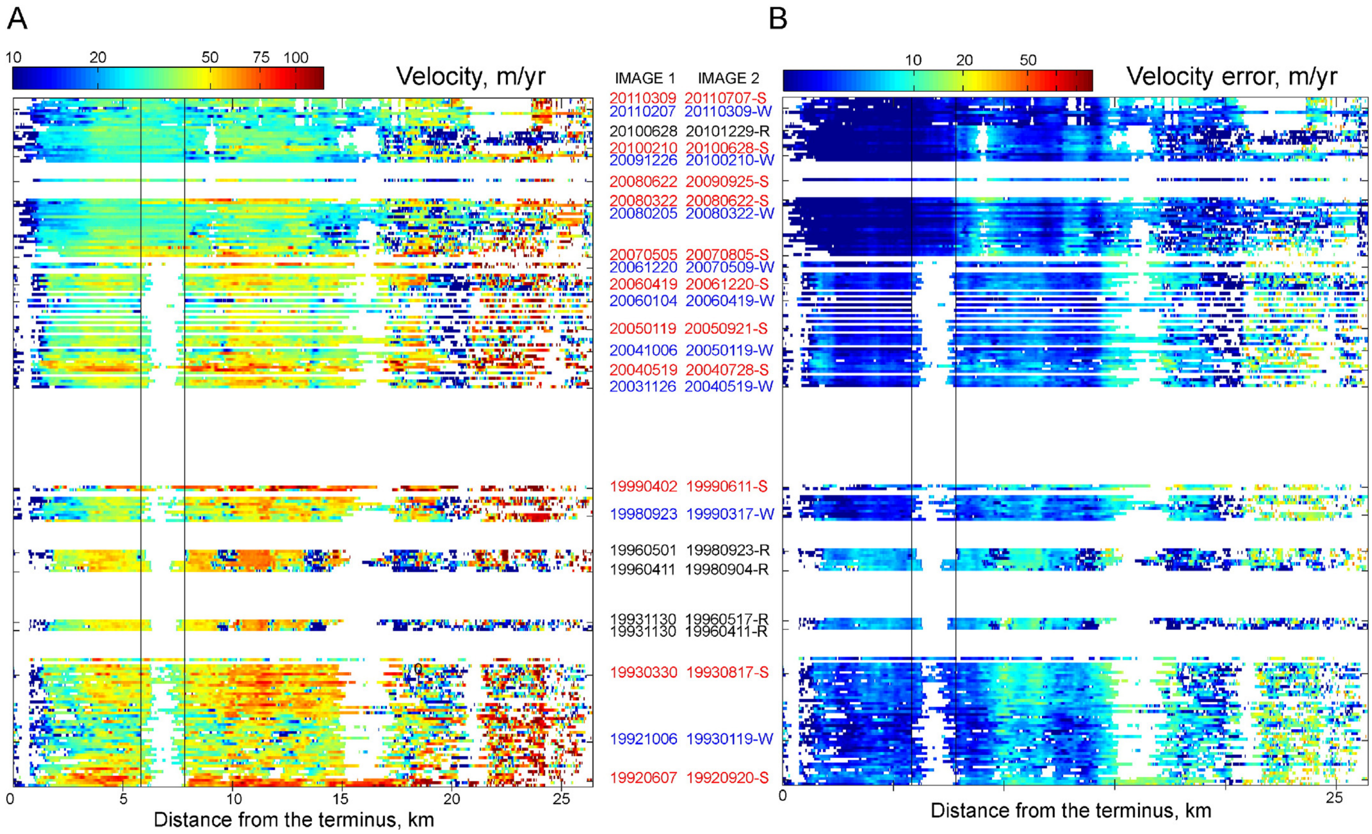

Fig. 5. Center line profiles of (a) surface velocity and (b) measurement error (standard deviation) along the length of the glacier for the entire dataset (spanning 1992–2011). Each profile is represented as a color coded strip, representing one pair of dates for which velocities were estimated. The vertical axis does not scale with time because of large gaps in temporal coverage (i.e. denser sampling during 1992–1993 and 2004–2011). This was necessary to depict at a glance all the velocity profiles in one figure. The gaps between strips represent time intervals with no data. The text on the y-axis are the dates of image pairs correspond to the peak summer and minimum winter velocities in each year, except pairs that use images from 1996 have >2-year intervals. Gaps in each strip correspond to data points rejected/masked due to low SNR and/or poor alignment with glacier margins (see section on Error analysis), while the gaps around ~7 km correspond to points rejected as they lie within the layover regions in the corresponding SAR images. The vertical lines bracketing these indicate the layover mask applied uniformly to all the data for the calculation of mean velocities of Figs. 6 & 7.

and 1999 which are separated by similar intervals. The peak summer speedup velocity in 1993 was 58.4 ± 5.5 m/yr, which is a reduction from 114% 1992 to 98% in 1993 while the peak in 2005 was 42.1 ± 3.9 m/yr, which is a reduction from 126% in 2004 to 57% in 2005. These observations lead us to infer that the decreasing trend seen during 2004–2011 may not have occurred during 1992–1998; this inference is also substantiated from the absence of such a trend in annual velocities for the years 1992, ~1995, ~1997 with gaps of >2 years (Fig. S3). The data points in 1995 and 1997 (Fig. S3), which are velocities averaged over 1993–1996 and 1996–1998 and which do not include the time when the peak summer velocities occurred in 1992–1993 and 1999, and allow us to infer that summer speedups of similar or larger magnitude may have occurred in the intervening years between 1993 and 1999. These observations suggest that the reducing trend of peak summer speedups during 2004–2011 may be unique over the observation period.

The inhomogeneous image acquisition times in our data could in principle have introduced two types of biases or artifacts. First, the peak velocity estimates might have missed the true peak due to inadequate sampling times or might be smaller because of being averaged over a long temporal window. Thus, our estimates of summer buildup may represent a lower bound on the true peak velocities. Second, the decreasing summer speedup from 2004 onwards could arise due to longer temporal baselines in later years. This is unlikely because the same pattern of decreasing velocities was observed even in periods with dense sampling (e.g. 2004 & 2007; Fig. 7). This is also substantiated by the fact that annual velocity estimates - which have longer temporal baselines and therefore relatively less affected by such a bias - also show a decreasing trend over the years (Fig. 7).

4. Discussion

This study characterized the spatiotemporal fluctuations in surface velocity over the Gangotri glacier during a period of nearly two decades (1992–2011). The results indicate relatively stable glacier wide winter velocities over the observation period, consistent intra-annual / seasonal fluctuations wherein surface velocity increases by nearly two-fold in summer and an inter-annual trend of decreasing summer speedup during the period 2004–2011. Below we interpret these findings in context of the existing literature on the Gangotri and other glaciers, and discuss how these observations elucidate its dynamics.

4.1. Surface velocity and overall glacier health

The surface velocities reported in this study are consistent with previous observations (Scherler et al., 2008; Scherler, Bookhagen, & Strecker, 2011b). However, no previous study has directly estimated seasonal and inter-annual variations. Also, the extensive literature on terminus retreat measurements for the Gangotri glacier warrants a comparison with the surface velocities near the terminus, which were only available for a few pairs from the L-band ALOS-PALSAR data. The surface velocities estimated within 0.5 km of the terminus in our study (4.2–5.8 ± 1 m/yr during 2007–2011) are in striking agreement with terminus retreat rates of ~5 m/yr measured during the last decade by several studies (see

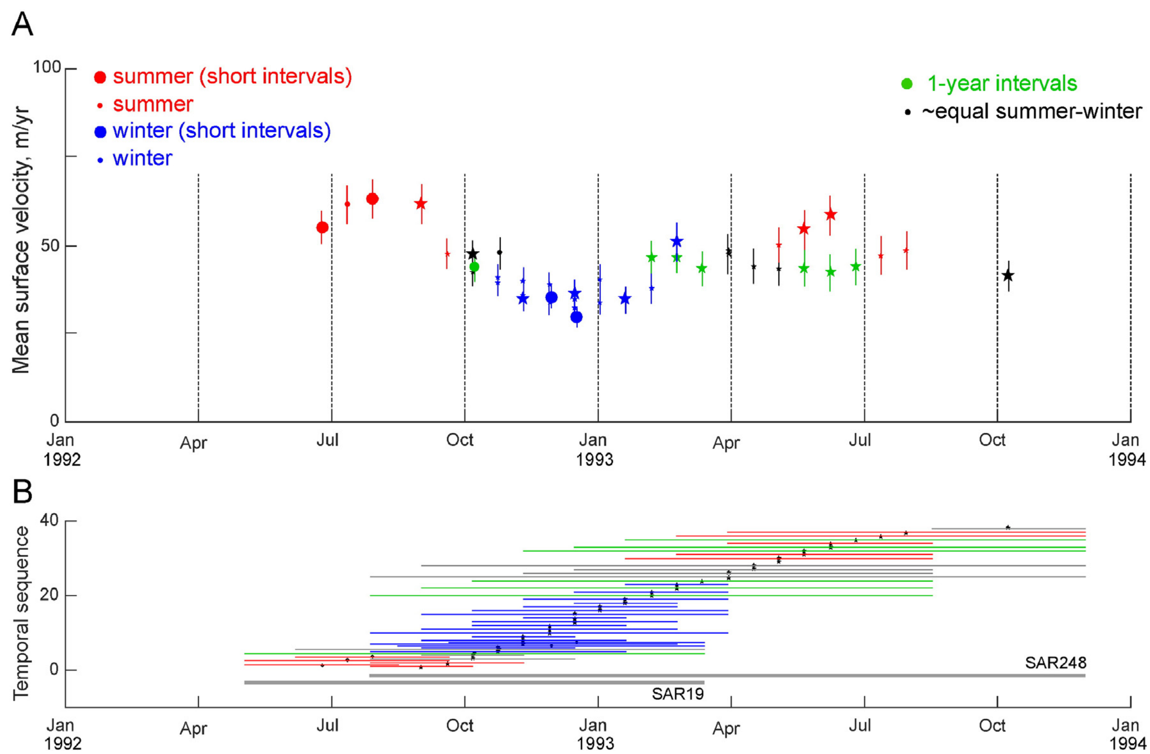

Fig. 6. Temporal evolution of surface velocity for the Gangotri glacier during 1992–1993. (A) Each point represents the mean surface velocity within the ablation region of the Gangotri glacier (0–12.6 km from the terminus) from one image pair with dates represented in (B) and mean standard deviation by error bars. Stars and circles represent data from satellites ERS248 and ERS19 respectively. Each line in (B) represents the start and end dates for image pairs matching the data in (A).

Fig. S2; Raina, 2009; Kumar et al., 2008; Kargel et al., 2011; Scherler et al., 2011a). Such concomitant changes in winter velocities with retreat/advance have been observed in field studies as well as from satellite images (Herman, Anderson, & Leprince, 2011; Vincent, Soruco, Six, & Le Meur, 2009).

My results show that the Gangotri glacier is dynamic throughout its length, with stable winter surface velocity that is high near the terminus region and increases to a maximum at ~25 km up-glacier. Such a velocity profile indicates an active glacier, as has been observed for other glaciers in the Himalayan region (Copland et al., 2009; Quincey et al.,

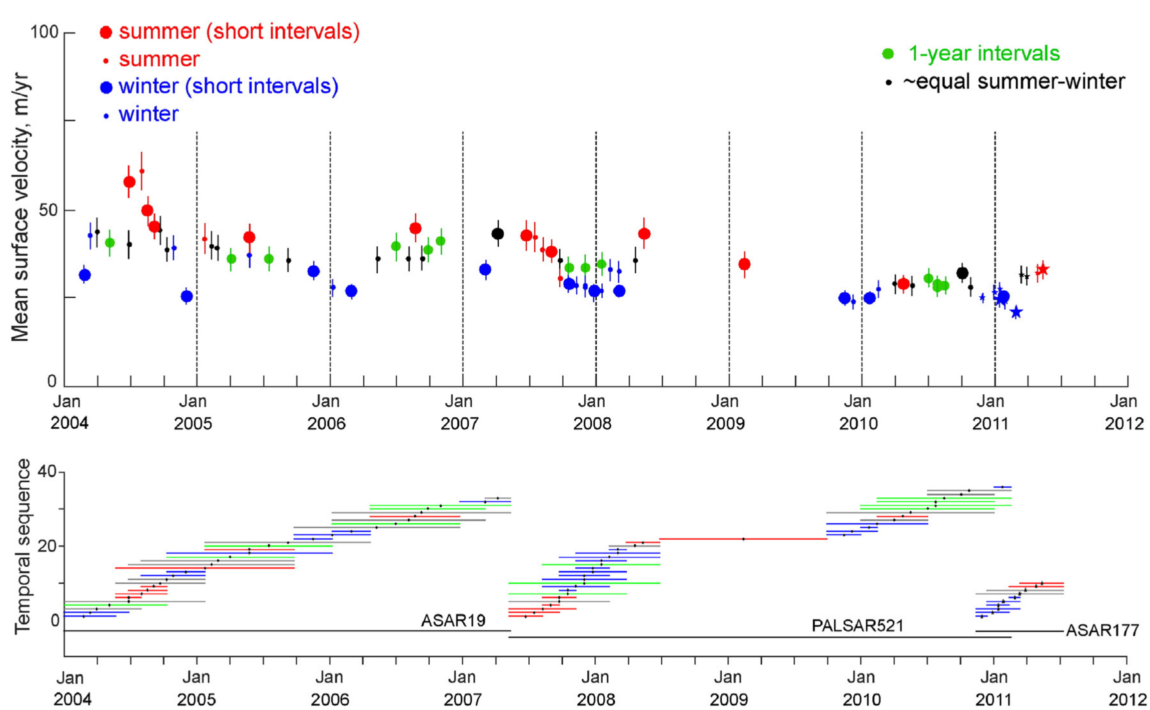

Fig. 7. Temporal evolution of surface velocity for the Gangotri glacier during 2004–2011. All conventions as in Fig. 6.

2009a; Quincey et al., 2009b; Scherler & Strecker, 2012). The overall shape of the down-glacier velocity profile is of the type classified by Scherler, Bookhagen, and Strecker (2011b) as a temperate glacier predominantly fed by avalanches with abundant debris cover and flow velocities that are highly skewed toward their headwalls. Glaciers in equilibrium tend to have convex-up elevation profiles in the ablation region and concave-up in the accumulation region (Anderson & Anderson, 2010). The Gangotri glacier elevation has such a shape almost up to the head wall at ~5505 m asl. All these observations indicate that the Gangotri glacier may be in a state of dynamic equilibrium. In contrast, downwasting glaciers in the Himalaya show long, stagnant tongues of near-zero velocities and concave-up elevation profiles in their ablation zones (Benn et al., 2012; Luckman et al., 2007; Quincey et al., 2009a).

Although terminus retreat, glacier thinning and reducing area of the Gangotri glacier have been taken as signs of its decline (Bhambri & Bolch, 2009; Bhambri et al., 2011a, 2012; Kargel et al., 2011), their glaciological significance (e.g. mass balance condition of the glacier) remains unclear. For example, Benn et al. (2012) have given a conceptual model of the evolution of debris-covered glaciers (as is Gangotri Glacier) during periods of negative mass balance, in the first stage of which all parts of the glacier are dynamically active. Given the paucity of diagnostic data, such of mass balance conditions for the Gangotri glacier and debris thickness/ablation rates over the length of the glacier, our finding that the glacier is dynamic throughout its length over a period of two decades (1992–2011) indicates that the Gangotri glacier is at worst in the first stage of decline or is still healthy.

4.2. Relation between surface velocity and subglacial processes

The surface velocity of glaciers is known to vary over multiple time scales (sub-daily to seasonal to inter-annual). The Gangotri glacier exhibited seasonal fluctuations with consistent summer speedup of ~60–120% during the years 1992–1993, 1998–1999, 2004–2011 (Figs. 5-7; Fig. S3 for 1996, 1998–1999) and inter-annual reduction of peak summer speedup following the peak in 2004 during the subsequent years till 2011, akin to other glaciers (Heinrichs, Mayo, Echelmeyer, & Harrison, 1996; Hodge, 1974; Iken & Truffer, 1997; Quincey et al., 2009a; Quincey et al., 2009b; Scherler & Strecker, 2012). Surface velocity fluctuations have been interpreted as a fluctuation in basal sliding (Willis, 1995) and elucidate many important internal dynamics of the Gangotri glacier as detailed below.

Variations in surface velocity of a glacier on these time scales are driven by changes in the subglacial drainage system. When melt–water percolates into a highly distributed subglacial drainage system, it causes an increase in pressure at the glacier bed, effectively lubricating it and resulting in increased basal sliding and surface velocity (Flowers, 2015; Fountain & Walder, 1998). But when melt–water is efficiently drained out through a channelized subglacial drainage system, it results in reduced basal sliding.

Englacial, subglacial and supraglacial melt water flows out of the glacier in the form of proglacial melt–water discharge from its terminus region. A high rate of melt–water discharge is accompanied by high rate and quantity of sediment flux in glaciers exhibiting basal sliding due to changes in bed hydrology (e.g. Anderson et al., 2004; Riihimaki, MacGregor, Anderson, Anderson, & Loso, 2005). Measurements of suspended sediment concentration (SSC) can therefore provide valuable insights into the sliding history of the glacier and ultimately, the dynamics of the subglacial drainage system (Riihimaki et al., 2005).

Thus, surface velocity and meltwater discharge are independently measurable quantities that are intimately linked to the subglacial drainage system of the glacier, the key player in driving seasonal and inter-annual variations.

We interpret the observed substantial summer speedup in the surface velocity of the Gangotri glacier as indicative of increased basal sliding (Echelmeyer & Harrison, 1990; Willis, 1995). This is also supported by the fact that sediments in the proglacial melt–water have been traced to the erosion of bedrock from glacier movement (Haritashya et al., 2010), which typically accompanies basal sliding. The gradual reduction of peak summer speed attained in early melt season to winter levels implies that the subglacial drainage system evolves through the melt season, from a distributed to channelized system, resulting in a reduction of basal sliding (Anderson et al., 2004; Bartholomaus, Anderson, & Anderson, 2008; Fountain & Walder, 1998; Mair, Nienow, Sharp, Wohlleben, & Willis, 2002). Such an evolution of the drainage system over the melt season has also been inferred from analyses of delaying and storage characteristics of meltwater runoff near the snout of the Gangotri glacier (Singh et al., 2006).

We interpret the inter-annual trend in surface velocity (Fig. 7), with a peak summer speedup in 2004, followed by reduced speedup in the subsequent ~7 years (2005–2011) as reflecting the hydrodynamic coupling of the subglacial drainage system between winter and melt-seasons (Burgess, Larsen, & Forster, 2013; Heinrichs et al., 1996; Sole et al., 2013). This reduction could occur for two reasons: either due to reduced availability of melt–water or due to the formation of increasingly efficient melt–water channels, both of which could lead to lesser lubrication of the glacier-bed interface in each subsequent year. The former is unlikely given the melt–water availability indicated by proglacial discharge measurements (Arora, Kumar, Kumar, & Malhotra, 2014; Haritashya et al., 2006, 2010). We therefore conclude that the inter-annual reduction arises from the formation of increasingly efficient melt–water channels, as observed elsewhere (Anderson et al., 2004; Bartholomaus et al., 2008). This possibility is further supported by the fact that large summer velocities were generally followed by lower winter velocity in our data (Fig. 7; see Burgess et al., 2013).

Finally, the observed peak in summer speedup of 2004 is in striking correspondence with that of an unusually large rate and quantity of melt–water discharge and suspended sediment concentration (SSC) in 2004 compared to subsequent years (Haritashya et al., 2006, 2010), both of which are characteristic of glaciers exhibiting basal sliding due to changes in bed hydrology (e.g. Anderson et al., 2004; Riihimaki et al., 2005). We interpret the peaks in summer speedup and discharge measurements in 2004, as being due to induced basal motion arising from the anomalous rate of meltwater input rather than the volume (Bartholomaus et al., 2008; Schoof, 2010).

To what extent is surface velocity of the Gangotri Glacier correlated with the prevailing weather conditions? Temperature and melt–water discharge are well correlated Gangotri glacier, suggesting that melting of the glacier and sediment evacuation are temperature driven (Haritashya et al., 2006; Haritashya et al., 2010). However, as detailed above, the rate, quantity and storage of melt–water have different effects on the subglacial drainage system, which in turn affects surface velocity. The long term trends in surface velocity of the Gangotri glacier demonstrate an inter-annual coupling of its drainage system between summers and winters which precludes a simple relationship between surface velocity and climate.

5. Conclusions

In this study, I have characterized the spatiotemporal fluctuations in the surface velocity of the Gangotri glacier during the periods 1992–1993, 1998–1999 and 2004–2011. The main findings of this study are that the Gangotri Glacier is dynamic throughout its length with surface velocity that exhibits stable spatial variations, and seasonal and inter-annual fluctuations. The summer speed-up in surface velocity is indicative of basal sliding. The seasonal fluctuations in summer speed-up indicate a subglacial drainage system that becomes progressively better connected with advancing melt season, reducing basal sliding so that the surface velocity is brought back to winter levels by the end of the melt-period. The inter-annual reduction in peak summer speedup from 2004 to 2011 indicates an increasingly efficient subglacial drainage system during summers, with inter-annual hydrodynamic coupling between winters and melt-seasons.

Acknowledgements

I thank Vinod Gaur, V. K. Raina, J. Srinivasan and S.P. Arun for discussions. I also thank the two anonymous reviewers for raising many important issues that have helped improve the manuscript. This research has been funded by the Department of Science and Technology (DST), Government of India, New Delhi (grant #SR/DGH-22/2010) and the Council for Scientific and Industrial Research (CSIR), New Delhi (grant # 21(890)/12/EMR-II). Some of the Synthetic Aperture Radar data were provided by the European Space Agency through Category-1 project #8609. I am grateful to the National Geophysical Research Institute, Hyderabad and the Divecha Center for Climate Change & the Center for Atmospheric and Oceanic Sciences, Indian Institute of Science, Bangalore for providing the facilities to carry out this work.

Appendix A. Supplementary data

Supplementary data to this article can be found online at http://dx.doi.org/10.1016/j.rse.2016.03.042.

References

Anderson, R. S., & Anderson, S. P. (2010). Glaciers and glacial geology. *Chapter 8 in geomorphology: The mechanics and chemistry of landscapes (Cambridge University Press) textbook* (640 pp., published June 2010).

Anderson, R. S., Anderson, S. P., MacGregor, K. R., Waddington, E. D., O'Neel, S., Riihimaki, C. A., & Loso, M. G. (2004). Strong feedbacks between hydrology and sliding of a small alpine glacier. *Journal of Geophysical Research*, *109*, F03005.

Arora, Manohar, Kumar, R., Kumar, N., & Malhotra, J. (2014). Assessment of suspended sediment concentration and load from a large Himalayan glacier. *Hydrology Research*, *45*(2), 292–306. http://dx.doi.org/10.2166/nh.2013.129.

Bartholomaus, T. C., Anderson, R. S., & Anderson, S. P. (2008). Response of glacier basal motion to transient water storage. *Nature Geoscience*, *1*(1), 33–37.

Benn, D., Bolch, T., Hands, K., Gulley, J., Luckman, A., Nicholson, L., ... Wiseman, S. (2012). Response of debris-covered glaciers in the Mount Everest region to recent warming, and implications for outburst flood hazards. *Earth-Science Reviews*, *114*, 156–174. http://dx.doi.org/10.1016/j.earscirev.2012.03.008.

Bhambri, R., & Bolch, T. (2009). Glacier mapping: a review with special reference to the Indian Himalayas. *Progress in Physical Geography*, *33*(5), 672–704.

Bhambri, R., Bolch, T., & Chaujar, R. K. (2011b). Mapping of debris covered glaciers in the Garhwal Himalayas using ASTER DEMs and thermal data. *International Journal of Remote Sensing*, *32*(23), 8095–8119.

Bhambri, R., Bolch, T., & Chaujar, R. K. (2012). Frontal recession of Gangotri Glacier, Garhwal Himalayas, from 1965–2006, measured through high resolution remote sensing data. *Current Science*, *102*(3), 489–494.

Bhambri, R., Bolch, T., Chaujar, R. K., & Kulshreshtha, S. C. (2011a). Glacier changes in the Garhwal Himalaya, India, from 1968 to 2006 based on remote sensing. *Journal of Glaciology*, *57*(203), 543–556.

Burgess, E. W., Larsen, C. F., & Forster, R. (2013). Summer melt regulates winter glacier flow speeds throughout Alaska. *Geophysical Research Letters*, *40*, 6160–6164. http://dx.doi.org/10.1002/2013GL058228.

Copland, L., Pope, S., Bishop, M., Schroder, J. F., Jr., Clendon, P., Bush, A., ... Owen, L. (2009). Glacier velocities across the central Karakoram. *Annals of Glaciology*, *50*(52), 41–49.

Echelmeyer, K., & Harrison, W. D. (1990). Jakobshavns Isbrae, West Greenland: Seasonal variations in velocity — Or lack thereof. *Journal of Glaciology*, *36*, 82–88.

Flowers, G. E. (2015). Modeling water flow under glaciers and ice sheets. *Proceedings Royal Society A*, *471*, 20140907. http://dx.doi.org/10.1098/rspa.2014.0907.

Fountain, A. G., & Walder, J. S. (1998). Water flow through temperate glaciers. *Reviews of Geophysics*, *36*(3), 299–328.

Gantayat, P., Kulkarni, A. V., & Srinivasan, J. (2014). Estimation of ice thickness using surface velocities and slope: Case study at Gangotri Glacier, India. *Journal of Glaciology*, *60*(220), 277.

Gudmundsson, G. H. (1997a). Ice deformation at the confluence of two glaciers investigated with conceptual map-plane and flowline models. *Journal of Glaciology*, *43*, 537–547.

Gudmundsson, G. H., Iken, A., & Funk, Martin (1997b). Measurements of ice deformation at the confluence area of Unteraargletscher, Bernese Alps, Switzerland. *Journal of Glaciology*, *43*(145), 548–5556.

Harbor, J. M. (1992). Application of a general sliding law to simulating flow in a glacier cross-section. *Journal of Glaciology*, *38*, 182–190.

Haritashya, U. K., Kumar, A., & Singh, P. (2010). Particle size characteristics of suspended sediment transported in meltwater from the Gangotri Glacier, central Himalaya — An indicator of subglacial sediment evacuation. *Geomorphology*, *122*, 140–152.

Haritashya, U. K., Singh, P., Kumar, N., & Gupta, R. P. (2006). Suspended sediment from the Gangotri Glacier: Quantification, variability and associations with discharge and air temperature. *Journal of Hydrology*, *321*, 116–130.

Heinrichs, T. A., Mayo, L. R., Echelmeyer, K. A., & Harrison, W. D. (1996). Quiescent-phase evolution of a surge-type glacier: Black Rapids Glacier, Alaska, USA. *Journal of Glaciology*, *42*(140), 110–122.

Herman, F., Anderson, B., & Leprince, S. (2011). Mountain glacier velocity variation during a retreat/advance cycle quantified using sub-pixel analysis of ASTER images. *Journal of Glaciology*, *57*(202), 197–207.

Hodge, Steven M. (1974). Variations in the sliding of a temperate glacier. *Journal of Glaciology*, *13*(69), 349–369.

Iken, A., & Truffer, M. (1997). The relationship between subglacial water pressure and velocity of Findelengletscher, Switzerland, during its advance and retreat. *Journal of Glaciology*, *43*(144), 328–338.

Jarvis, A., Reuter, H. I., Nelson, A., & Guevara, E. (2008). Hole-filled SRTM for the globe Version 4. (available from the CGIAR-CSI SRTM 90m Database) http://srtm.csi.cgiar.org

Kääb, A. (2005). Combination of SRTM3 and repeat ASTER data for deriving alpine glacier flow velocities in the Bhutan Himalaya. *Remote Sensing of Environment*, *94*(4), 463–474.

Kääb, Andreas, Etienne, Berthier, Christopher, Nuth, Julie, Gardelle, & Yves, Arnaud (2012). Contrasting patterns of early twenty-first-century glacier mass change in the Himalayas. *Nature*, *488*, 495–498.

Kargel, J. S., Cogley, J. G., Lenoard, G. J., Haritashya, U., & Byers, A. (2011). Himalayan glaciers: The big picture is a montage. *Proceedings of the National Academy of Sciences*, *108*(36), 14709–14710.

Kennet (2014). *Glaciers of the Karakorum Himalaya, glacial environments, processes, hazards and resources.* (book) Springer.

Kobayashi, T., Takada, T., Furuya, M., & Murakami, M. (2009). Locations and types of ruptures involved in the 2008 Sichuan earthquake inferred from SAR image matching. *Geophysical Research Letters*, *36*, L07302. http://dx.doi.org/10.1029/2008GL036907.

Kumar, K., Dumka, R. K., Miral, M. S., Satyal, G. S., & Pant, M. (2008). Estimation of retreat rate of Gangotri glacier using rapid static and kinematic GPS survey. *Current Science*, *94*, 258–262.

Kumar, Vijay, Venkataraman, Gopalan, Høgda, Kjell Arild, & Larsen, Yngvar (2013). Estimation and validation of glacier surface motion in the north-western Himalayas using high-resolution SAR intensity tracking. *International Journal of Remote Sensing*, *34*(15), 5518–5529.

Luckman, A., Quincey, D. J., & Bevan, S. (2007). The potential of satellite radar interferometry and feature tracking for monitoring flow rates of Himalayan glaciers. *Remote Sensing of Environment*, *111*(2–3), 172–181.

Mair, D., Nienow, P., Sharp, M., Wohlleben, T., & Willis, I. (2002). Influence of subglacial drainage system evolution on glacier surface motion: Haut Glacier d'Arolla, Switzerland. *Journal Geophysical Research*, *107*(B8), 1–13. http://dx.doi.org/10.1029/2001JB000514 (EPM 8).

Naithani, A. K., Nainwal, H. C., Sati, K. K., & Prasad, C. (2001). Geomorphological evidences of retreat of the Gangotri glacier and its characteristics. *Current Science*, *80*, 87–94.

Pratap, B., Dobhal, Dwarika Prasad, Bhambri, Rakesh, Mehta, Manish, & Tewari, Vinod Chandra (2015). Four decades of glacier mass balance observations in the Indian Himalaya. *Regional Environmental Change*. http://dx.doi.org/10.1007/s10113-015-0791-4.

Pritchard, H., Murray, T., Luckman, A., Strozzi, T., & Barr, S. (2005). Glacier surge dynamics of Sortebræ, east Greenland, from synthetic aperture radar feature tracking. *Journal of Geophysical Research*, *110*, F03005. http://dx.doi.org/10.1029/2004JF000233.

Quincey, D. J., Copland, L., Mayer, C., Bishop, M., Luckman, A., & Belò, M. (2009a). Ice velocity and climate variations for the Baltoro Glacier, Pakistan. *Journal of Glaciology*, *55*, 1061–1071. http://dx.doi.org/10.3189/002214309790794913.

Quincey, D. J., Luckman, A., & Benn, D. I. (2009b). Quantification of Everest region glacier velocities between 1992 and 2002, using satellite radar Interferometry and feature tracking. *Journal of Glaciology*, *55*, 596–606.

Rabus, R. T., & Fatland, D. R. (2000). Comparison of SAR-Interferometric and surveyed velocities on a mountain glacier: Black Rapids Glacier, Alaska, U.S.A. *Journal of Glaciology*, *46*(152), 119–128.

Raina, V. K. (2009). Himalayan glaciers: A state-of-art review of glacial studies, glacial retreat and climate change. *Discussion paper*. New Delhi: Ministry of Environment and Forests, Government of India.

Rignot, E., Echelmeyer, K., & Krabill, W. (2001). Penetration depth of Interferometric synthetic-aperture radar signals in snow and ice. *Geophysical Research Letters*, *28*(18), 3501–3504.

Riihimaki, C. A., MacGregor, K. R., Anderson, R. S., Anderson, S. P., & Loso, M. G. (2005). Sediment evacuation and glacial erosion rates at a small alpine glacier. *Journal of Geophysical Research*, *110*, F03003. http://dx.doi.org/10.1029/2004JF000189.

Saraswat, Puneet, Syed, Tajdarul H., Famiglietti, James S., Fielding, Eric J., Crippen, Robert, & Gupta, Nishant (2013). Recent changes in the snout position and surface velocity of Gangotri glacier observed from space. *International Journal of Remote Sensing*, *34*(24), 8653–8668.

Scherler, D., & Strecker, M. R. (2012). Large surface velocity fluctuations of Biafo Glacier, central Karakorum, at high spatial and temporal resolution from optical satellite images. *Journal of Glaciology*, *58*(209), 2012. http://dx.doi.org/10.3189/2012JoG11J096.

Scherler, D., Leprince, S., & Strecker, M. R. (2008). Glacier-surface velocities in alpine terrain from optical satellite imagery: Accuracy improvement and quality assessment. *Remote Sensing of Environment*, *112*(10), 3806–3819. http://dx.doi.org/10.1016/j.rse.2008.05.018.

Scherler, D., Bookhagen, B., & Strecker, M. R. (2011a). Spatially variable response of Himalayan glaciers to climate change affected by debris cover. *Nature Geoscience*, *4*, 156–159.

Scherler, D., Bookhagen, B., & Strecker, M. R. (2011b). Hillslope–glacier coupling: The interplay of topography and glacial dynamics in High Asia. *Journal of Geophysical Research*, *116*, F02019. http://dx.doi.org/10.1029/2010JF001751.

Schoof, C. (2010). Ice-sheet acceleration driven by melt supply variability. *Nature*, *468*, 803–806. http://dx.doi.org/10.1038/nature09618.

Singh, P., Haritashya, U. K., Kumar, N., & Singh, Y. (2006). Hydrological characteristics of the Gangotri Glacier, Central Himalayas, India. *Journal of Hydrology*, *327*(1–2), 55–67.

Sole, A., Nienow, P., Bartholomew, I., Mair, D., Cowton, T., Tedstone, A., & King, M. A. (2013). Winter motion mediates dynamic response of the Greenland Ice Sheet to warmer summers. *Geophysical Research Letters*, *40*, 3940–3944. http://dx.doi.org/10.1002/grl.50764.

Srivastava, D. (2012). Status report on Gangotri glacier, Science and Engineering Research Board, Department of Science and Technology, New Delhi. *Himalayan glaciology technical report no. 3* (102 pp.).

Strozzi, T., Luckman, A., Murray, T., Wegmüller, U., & Werner, C. (2002). Glacier motion estimation using SAR offset-tracking procedures. *IEEE Transactions on Geoscience and Remote Sensing*, *40*(11), 2384–2391.

Vincent, C., Soruco, A., Six, D., & Le Meur, E. (2009). Glacier thickening and decay analysis from 50 years of glaciological observations performed on Glacier d'Argentie`re, Mont Blanc area, France. *Annals of Glaciology*, *50*, 73–79.

Willis, I. C. (1995). Intra-annual variations in glacier motion, a review. *Progress in Physical Geography*, *19*, 61–106.

Yasuda, T., & Furuya, M. (2013). Short-term glacier velocity changes at West Kunlun Shan, Northwest Tibet, detected by synthetic aperture radar data. *Remote Sensing of Environment*, *128*, 87–106.